International Journal on Magnetic Particle Imaging
Vol 8, No 1, Suppl 1, Article ID 2203084, 4 Pages

Infinite Science Publishing

Proceedings Article

VivoTrax+™ improves the detection of cancer cells with magnetic particle imaging

J. J. Gevaert[a,b,*] · K. Van Beek[a] · O. C. Sehl[a,b] · P. J. Foster[a,b]

[a]Department of Medical Biophysics, University of Western Ontario, London, Canada
[b]Cellular and Molecular Imaging Group, Robarts Research Institute, London, Canada
[*]Corresponding author, email: jgevaert@uwo.ca

Abstract

Cellular imaging is a rapidly growing field as novel tracers and imaging techniques are developed. Magnetic particle imaging (MPI) detects superparamagnetic iron oxide nanoparticles (SPIO), which can be used to label cells. The unique detection of SPIO-labeled cells boasts MPI as a sensitive modality; as such, the type of SPIO has a critical role in determining sensitivity and resolution. For cell tracking applications, the ideal SPIO should label cells efficiently and retain its sensitivity after cellular uptake. VivoTrax™, a commercially available and commonly used SPIO for MPI, was recently re-released as VivoTrax+™ with an improved size distribution enriched for larger particles. In this study, VivoTrax+™ is shown to enhance cellular labeling and improve in vitro/in vivo sensitivity. Importantly, the sensitivity of both SPIO significantly decreased after cellular internalization. The results from this study emphasize the importance of translating SPIO performance in vivo to maintain its utility for cell tracking applications.

I. Introduction

Cellular imaging can answer many fundamental questions about the presence, numbers, persistence, and delivery of cell therapies. Magnetic particle imaging (MPI) is a non-invasive, non-ionizing, sensitive modality capable of tracking cells labeled with superparamagnetic iron oxide nanoparticles (SPIO). Importantly, signal is proportional to iron content, which, combined with a measure of iron per cell, can be used to quantify cell number. As a tracer-based modality, the type of SPIO has a critical role in determining sensitivity and resolution. The ideal SPIO for cell tracking should label cells efficiently, without inducing cytotoxicity, and retain magnetic properties after cellular internalization.

VivoTrax™ (Magnetic Insight Inc.), or ferucarbotran, is a common MPI tracer and has been used to detect a variety of cell types [1-8]. Although widely used, it is not considered optimal for MPI due to its bimodal size distribution comprised of ~30% 25-30 nm cores and ~70% 5 nm cores [9,10]. The smaller cores do not magnetize sufficiently, leaving a small fraction of particles that contribute to signal. Recently, Magnetic Insight released VivoTrax+™, a filtered form of VivoTrax™ that increases the fraction of larger cores for improved MPI performance. This study directly compares the two agents by assessing sensitivity, cell labeling efficiency, and *in vivo* imaging.

II. Material and methods

II.I. Cell Labeling

A2058 human melanoma cancer cells were cultured at 37° in complete Dulbecco's modified Eagle's medium (Thermo Fisher Scientific, Waltham, Massachusetts) until 90% confluent. VivoTrax+™ and VivoTrax™ were added to separate cultures (200µg Fe/mL) either with protamine sulfate (0.24 mg/mL) and heparin (8 USP units/mL) as transfection agents (TAs), or without the

10.18416/ijmpi.2022.2203084

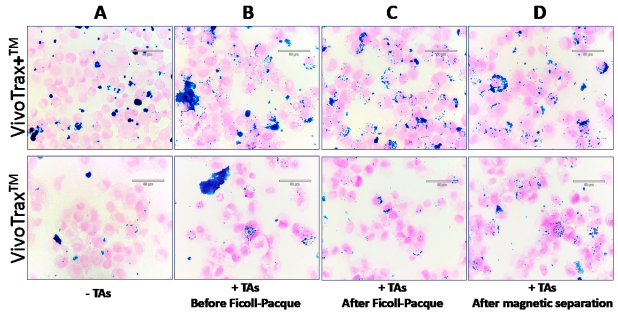

Figure 1: PPB of A2058 cancer cells labeled with VivoTrax+™ and VivoTrax™ (A) without TAs (B) with TAs (C) after Ficoll-Pacque and (D) after magnetic separation.

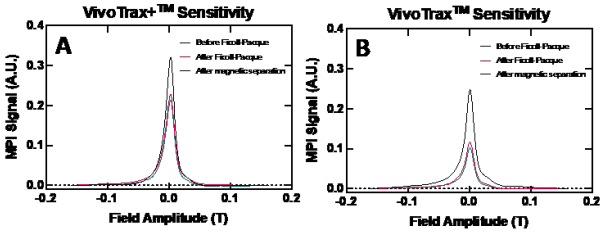

Figure 2: Relaxometry showing the signal of labeled cells before and after Ficoll-Pacque and after magnetic column separation for (A) VivoTrax+™ and (B) VivoTrax™.

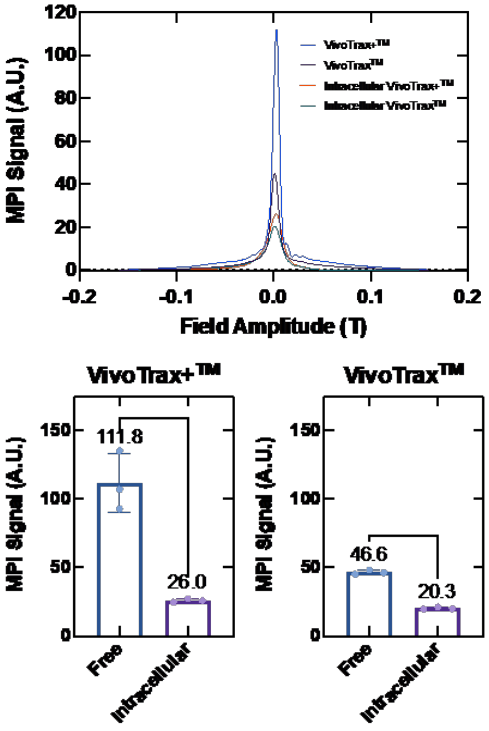

Figure 3: Signal of VivoTrax+™ and VivoTrax™ before (free) and after cellular uptake (intracellular).

addition of TAs. After overnight incubation, cells were washed 3 times with phosphate-buffered saline (PBS). Cell counting and viability was determined using the trypan-blue exclusion assay (Countess Automated Cell Counter; Invitrogen). Perls Prussian Blue (PPB) staining was then performed to assess iron labeling.

For cells labeled with TAs, Ficoll-Pacque density gradient separation was applied to remove remaining extracellular iron after PBS washing. Cells were suspended in 6 mL media and carefully layered over 3 mL Ficoll-Pacque in a 15 mL falcon tube then spun at 400 × *g* for 20 minutes without brakes. Cells were collected at the interface of the two solutions, then separation of labeled from unlabeled cells was conducted with a magnetic column. Cells were resuspended in 2 mL PBS and incubated for 5 minutes in an EasySep™ magnet (Stemcell Technologies, Vancouver, CAN) at room temperature. Flow through of unlabeled cells was discarded while SPIO+ cells remaining in the tube were collected.

At each labeling stage (before Ficoll-Pacque, after Ficoll-Pacque, and after magnetic column separation), PPB staining was performed and samples containing 1×10^6 cells suspended in ~250 µL PBS were collected for MPI acquisitions. Only cells labeled with TAs were used for further experiments.

II.II. *In vitro* and *In vivo* MPI Acquisitions

MPI relaxometry was performed on triplicate samples containing 1×10^6 VivoTrax+™ or VivoTrax™ labeled cells from each labeling stage using the RELAX™ module equipped on the Momentum™ scanner (Magnetic Insight Inc.). Relaxometry curves were analyzed using Prism software (9.3.0, GraphPad Inc.) for sensitivity values (peak signal) between the different labeling stages and to compare SPIO sensitivity before (free) and after cellular uptake (intracellular).

To assess the effects of extracellular iron on MPI signal, samples containing 62.5K, 31.3K, 15.6K, 7.8K, and 3.9K (K = 1000) VivoTrax+™ or VivoTrax™ labeled cells suspended in ~250 µL PBS were made from each labeling stage. Projection images were acquired in 2D with a 3.0 T/m selection field gradient and drive field strengths of 22 mT and 26 mT in the X and Z axes, respectively. These 2D images took ~2 minutes to acquire for a 12 x 6 cm field of view (FOV).

In vivo imaging was performed on nude mice 24 hours post intravenous (IV) injections of 40 µL (220 µg Fe) VivoTrax+™ (n = 3) and VivoTrax™ (n = 3). Prior to imaging, mice were fasted for 12 hours with only water, a laxative, and corn bedding in their cage, to reduce gastrointestinal signal. Mice were anesthetized with 2% isoflurane and maintained with 1% isoflurane during

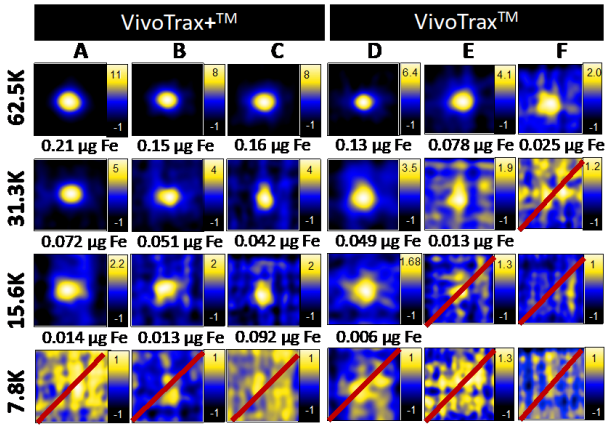

Figure 4: 2D MPI of cell samples (A, D – before Ficoll-Pacque, B, E – after Ficoll-Pacque, C, F – after magnetic separation).

imaging. The same image parameters were used for 3D imaging, which combines 35 projections (30 min).

All images were analyzed using open-source Horos™ image analysis software (version 3.3.6, Annapolis, MD USA). MPI signal was measured using a region of interest (ROI) that selects signals that exceed 5 times the standard deviation of system noise [11].

III. Results and discussion

III.I. VivoTrax+™ has a higher labeling efficiency

Without TAs, most iron remained extracellular with minimal uptake in cells for both VivoTrax+™ and VivoTrax™ (Fig. 1A). Adding TAs enhanced iron uptake in these less phagocytic cells (compared to macrophages), but also produced extracellular clumps of iron (Fig. 1B). Ficoll-Pacque efficiently removed extracellular iron (Fig. 1C). After magnetic separation, unlabeled cells were removed (Fig. 1D). Visually, panels C and D are similar indicating most cells were labeled and few were removed after magnetic separation. Qualitatively, VivoTrax+™ improved uptake in cells compared to VivoTrax™.

After Ficoll-Pacque, the MPI signal decreased by ~30% for VivoTrax+™ (Fig. 2A) and ~50% VivoTrax™ (Fig. 2B) because of extracellular iron being removed. There was no significant change in MPI signal after magnetic separation, indicating few cells were unlabeled. This result shows that extracellular iron will overestimate the MPI signal associated with cells, thus the Ficoll-Pacque technique may be critical for accurate quantification of labeled cells.

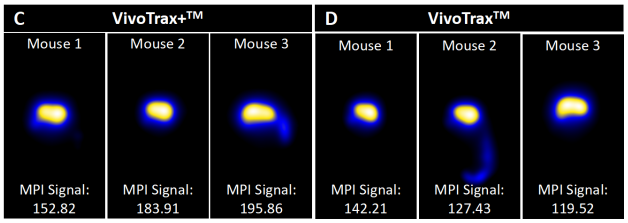

Figure 5: In vivo MPI signal of VivoTrax+™ and VivoTrax™ after IV injections in nude mice. Significantly more signal was detected in mice injected with VivoTrax+™ than VivoTrax™.

III.II. MPI signal decreases after cellular uptake

Relaxometry of free and intracellular VivoTrax+™ and VivoTrax™ is shown in Fig. 3. The MPI signal was ~2.4 times higher for free VivoTrax+™ compared to free VivoTrax™ (111.8 vs. 46.6). After cellular internalization, the signal was reduced by ~4 times for VivoTrax+™ and ~2 times for VivoTrax™. This has been shown to be related to the confined intracellular environment and aggregation of iron cores which slows relaxation [12-15]. This effect was greater for VivoTrax+™ and might be explained by larger aggregates forming inside the cell from a higher fraction of larger cores.

III.III. VivoTrax+™ improves cellular sensitivity

As few as 15.6K VivoTrax+™ labeled cells were detected using 2D imaging after all 3 labeling stages (Fig. 4A-C). With VivoTrax™, 15.6K cells were only visible before Ficoll-Pacque because of extracellular iron contributing to MPI signal (Fig. 4D). After extracellular iron was removed, MPI signal decreased, and only 31.3K cells were detected (Fig. 4E). After magnetic separation, there was a slight decrease in signal, and only as few as 62.5K cells were detected (Fig. 4F). This may be explained by the column removing lightly labeled cells. Overall, VivoTrax+™ detected fewer cells with improved labeling; 7.5 pg Fe/cell compared to VivoTrax™ with 4.2 pg Fe/cell. Extracellular iron prior to Ficoll-Pacque falsely contributed to cell signal with VivoTrax™, overestimating sensitivity.

III.IV. VivoTrax+™ improves *in vivo* sensitivity

Six nude mice were imaged with MPI following iv injected VivoTrax™ (n = 3) or VivoTrax+™ (n = 3) positioned as shown in Fig. 5A. MPI signal was observed in the mouse liver 24 hours post-injection, a result of uptake of iron by phagocytic Kupffer cells. Significantly more signal was detected in the livers of mice injected with VivoTrax+™

compared to VivoTrax™ (Fig. 5B-D), demonstrating improved *in vivo* sensitivity. Residual iron from the injection is seen in the tail for Mouse 2 (Fig. 5D).

IV. Conclusions

This study demonstrates the improved performance of VivoTrax+™ and its potential use for cell tracking applications. VivoTrax+™ had a higher labeling efficiency compared to VivoTrax™, using transfection agents as a labeling strategy to enhance cellular uptake. Furthermore, a higher cellular sensitivity was achieved, and significantly more MPI signal was detected in the liver of nude mice 24 hours post IV SPIO-injection. Cellular internalization significantly reduced the sensitivity of both SPIO, particularly with VivoTrax+™. This phenomenon impacts the magnetic relaxation properties of the SPIO after cell internalization, directly affecting MPI sensitivity and resolution. In addition to retaining magnetic properties, labeling cells efficiently is imperative for improving cellular sensitivity. With the rapid development of SPIO, these factors must be considered for cell tracking applications. This study paves a pathway for testing SPIO sensitivity initially as a free agent to its *in vitro* and *in vivo* performance, translating its utility to cell tracking applications.

Acknowledgments

We acknowledge funding from the National Sciences and Engineering Research Council.

Author's statement

Conflict of interest: Authors state no conflict of interest.

References

[1] H. Nejadnik, Ferumoxytol can be used for quantitative Magnetic Particle Imaging of Transplanted Stem Cells, Mol Imaging Biol, vol. 21(3), pp. 465-472, Jun. 2019.

[2] O.C. Sehl, Trimodal cell tracking in vivo: Combining iron- and fluorine-based magnetic resonance imaging with magnetic particle imaging to monitor the delivery of mesenchymal stem cells and the ensuing inflammation, Tomography, vol. 5(4), pp. 367–376, Dec. 2019.

[3] B. Zheng, Quantitative magnetic particle imaging monitors the transplantation, biodistribution, and clearance of stem cells in vivo, Theranostics, vol. 6, pp. 291–301, Jan. 2016.

[4] A.V. Makela, Quantifying tumor associated macrophages in breast cancer: a comparison of iron and fluorine-based MRI cell tracking. Sci. Rep., vol. 7, pp. 42109, Feb. 2017.

[5] J. Bulte, Quantitative "hot-spot" imaging of transplanted stem cells using superparamagnetic tracers and magnetic particle imaging, Tomography, vol. 1, pp. 91–97, Dec. 2015.
[6] P. Wang, Magnetic particle imaging of islet transplantation in the liver and under the kidney capsule in mouse models. Quant. Imaging Med. Surg., vol. 8, pp. 114–122, Mar. 2018.

[7] G. Song et al, Janus iron oxides @ semiconducting polymer nanoparticle tracer for cell tracking by magnetic particle imaging. Nano Lett., vol. 18, pp. 182–189. 2018.

[8] Q. Wang et al., Artificially engineered cubic iron oxide nanoparticle as a high-performance magnetic particle imaging tracer for stem cell tracking. ACS Nano., vol. 14, pp. 2053–2062. 2020.

[9] D. Eberbeck, Multicore magnetic nanoparticles for magnetic particle imaging. IEEE Trans. Magnetics, vol. 49, pp. 269–274, Jan. 2013.

[10] D. Eberbeck, How the size distribution of magnetic nanoparticles determines their magnetic particle imaging performance, Appl. Phys. Lett., vol. 98, pp. 182502, May. 2011.

[11] A. Rose, Human vison, in Vision. Optical Physics and Engineering, Springer, Boston, MA.

[12] H. Arami, Intracellular performance of tailored nanoparticle tracers in magnetic particle imaging. J. Appl. Phys., vol. 115, pp. 17B306, Mar. 2014.

[13] H. Suzuka, Magnetic nanoparticles in macrophages and cancer cells exhibit different signal behavior on magnetic particle imaging. J. Nanosci. Nanotechnol., vol. 19(11), pp. 6857-6865, Nov. 2019.

[14] H. Paysen, Cellular uptake of magnetic nanoparticles imaged and quantified by magnetic particle imaging, Sci. Rep., vol. 10, pp. 1922, Feb. 2020.

[15] E. Teeman, Intracellular dynamics of superparamagnetic iron oxide nanoparticles for magnetic particle imaging, Nanoscale, vol. 11, pp. 7771–7780, Mar. 2019.

